Nonlinear analysis of the emission of close binary supermassive black hole candidates

Andjelka Kovačević, Luka Č. Popović

University of Belgrade-Faculty of Mathematics

Emission-line dynamics

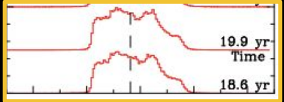

Bogdanović +09, Shen & Loeb +10; Popovic+21

tidal disruptions by a binary

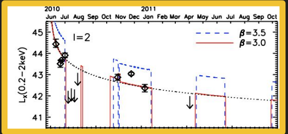

Liu, Li, Komossa+14 Huang+21

Jet morphology

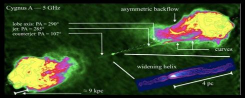

Gower +82, Krause +18

Periodic emission , lensing

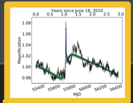

Graham+15, Hu+19

Time domain surveys

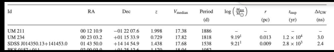

Graham+15, Liu+19, Guo+19

~>200 Binary SMBH candidates

timeline

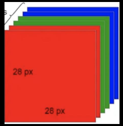

2D /3D tensors

Data tensors evolution

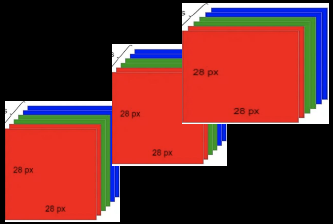

4D tensors

Active Galactic Nuclei (AGN)

AGNs are powered by the release of gravitational energy related with the accretion of material onto a supermassive black hole (SMBH), with masses larger than $10^6\,M_\odot$

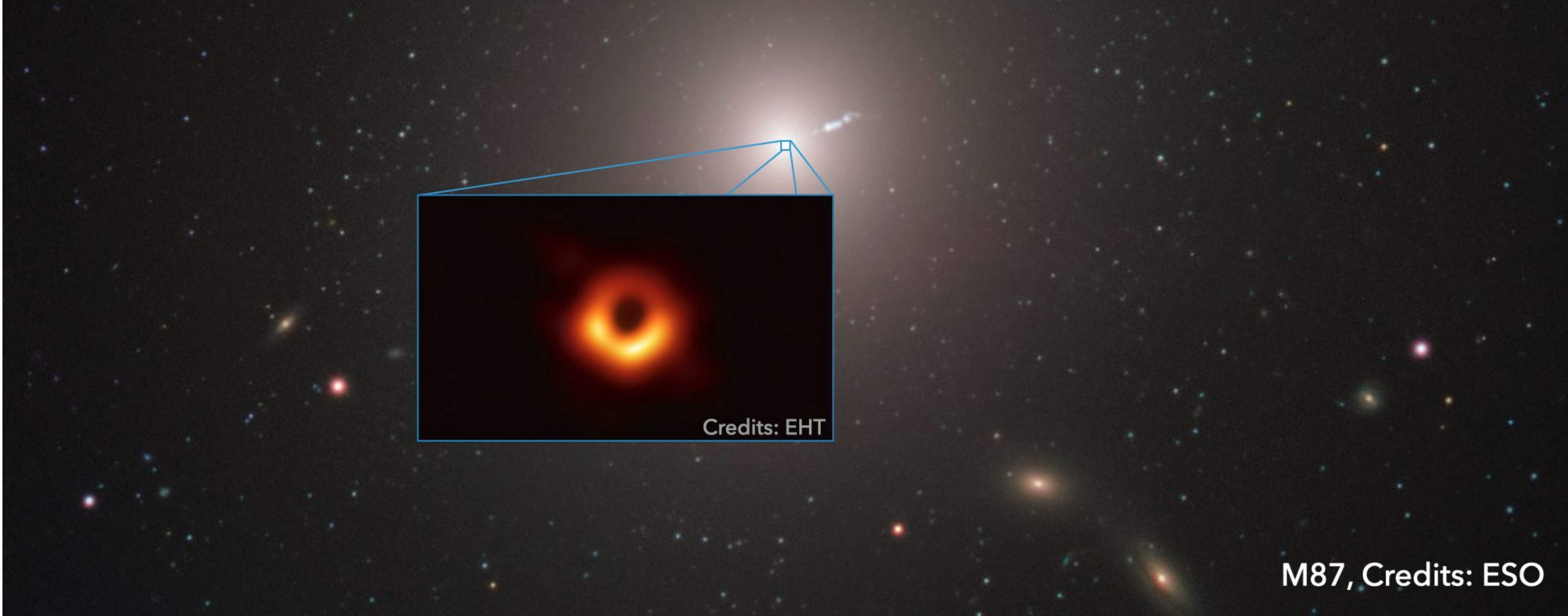

M87, Credits: ESO

Active Galactic Nuclei (AGN) - *ID card*

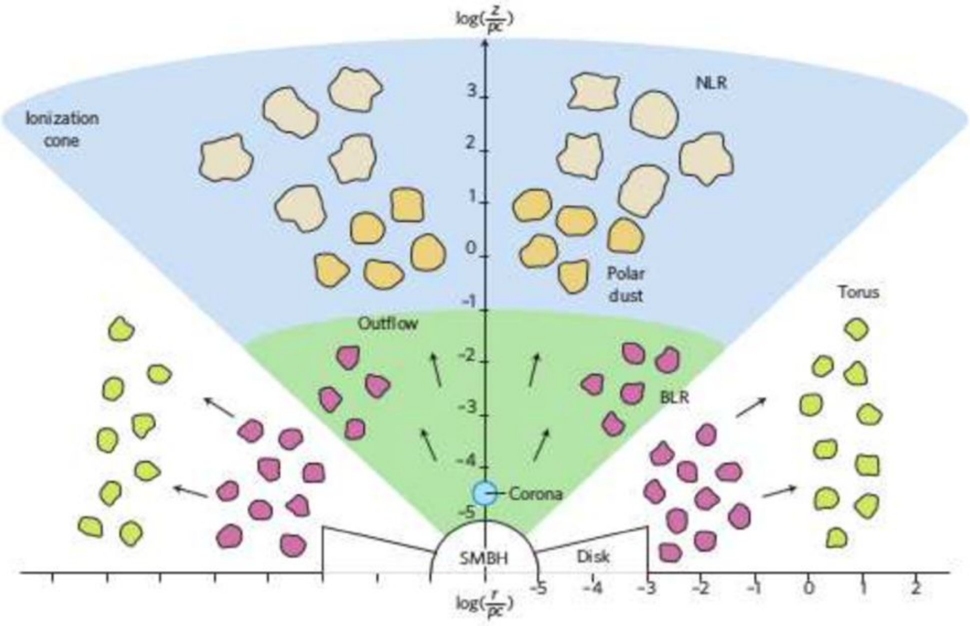

Ramos Almeida & Ricci (2017)

- **Black Hole Mass** $10^6 \lesssim M_{\rm BH} \lesssim 10^9\,(M_\odot)$
- **Luminosity** $10^{12} \lesssim L_{\rm AGN} \lesssim 10^{15}\,(L_\odot)$
- **Spin** $-1 \lesssim a_* \lesssim 1$
- **Accretion rate** $0.01 \lesssim \dot{M} \lesssim 10\,(M_\odot/{\rm yr})$
- **Eddington ratio** $0.01 \lesssim \dfrac{L}{L_{\rm Edd}} \lesssim 1$

$$\frac{L}{L_{\rm Edd}} \propto \frac{L_{\rm AGN}}{M_{\rm BH}}$$

How can we reveal the inner structure?

AGN variability: what do we know?

AGN variability seems to be well described as a **stochastic process**: behavior that is not predictable forever as in the periodic case, but unlike temporally localized events (transient), variability is always there

Stochastic | Periodic | Transient

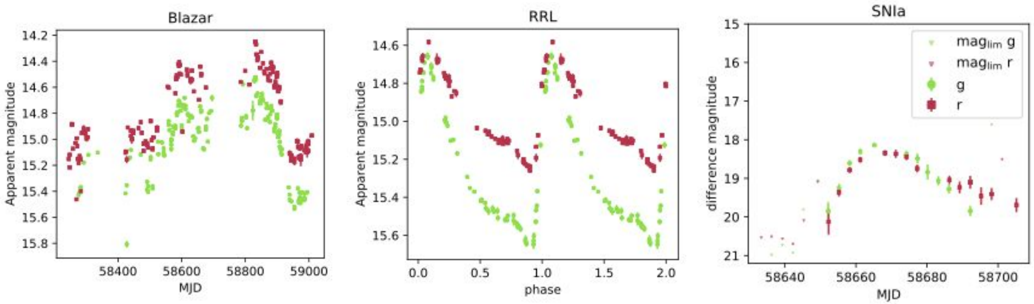

credits: Sánchez-Sáez et al. 2021a.

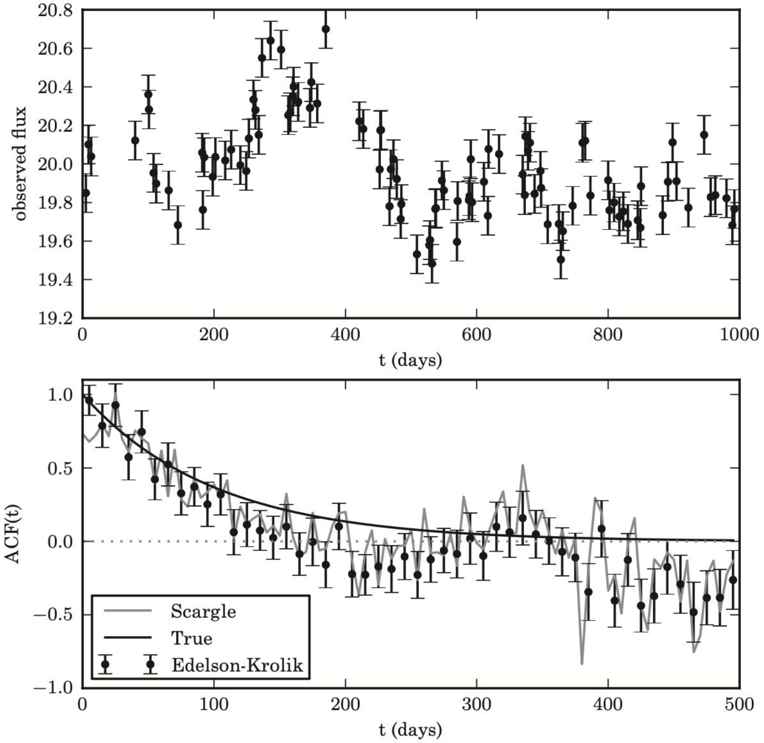

for more details see [Kozlowski et al. 2016]

fractals in time

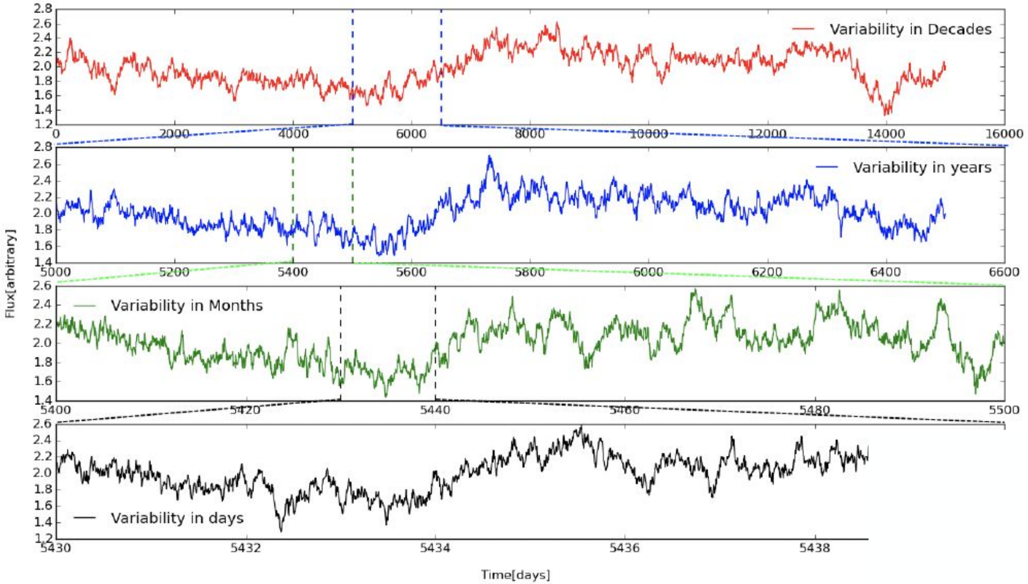

Astronomical red noise

1/f~fractals in time

Table 4.1 Nomenclature of noise spectra.

Power spectrum	Power index	Spectrum nomenclature
$P(\nu) \propto \nu^0$	$p = 0$	white noise
$P(\nu) \propto \nu^{-1}$	$p = 1$	pink noise, flicker noise, $1/f$ noise
$P(\nu) \propto \nu^{-2}$	$p = 2$	red noise, Brown(ian) noise
$P(\nu) \propto \nu^{-3}$	$p = 3$	black noise

Astronomical tomography

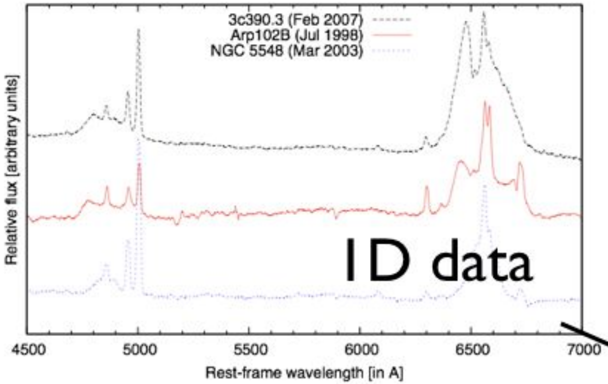

Figure 1: Examples of spectra of objects from our monitoring campaign: 3C 390.3, Arp 102B, and NGC 5548. The dates of observations are given in brackets.

1D data

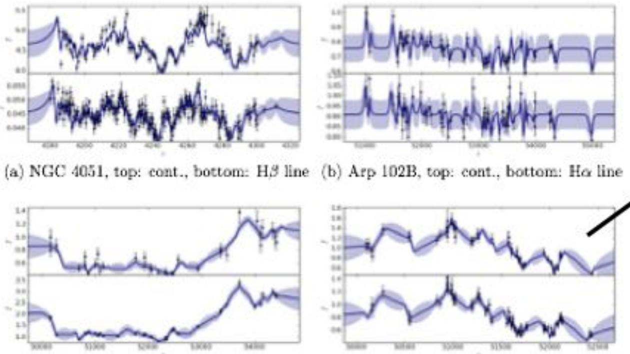

(a) NGC 4051, top: cont., bottom: Hβ line (b) Arp 102B, top: cont., bottom: Hα line

(c) 3C 390.3, top: cont., bottom: Hα line (d) NGC 5548, top: cont., bottom: Hβ line

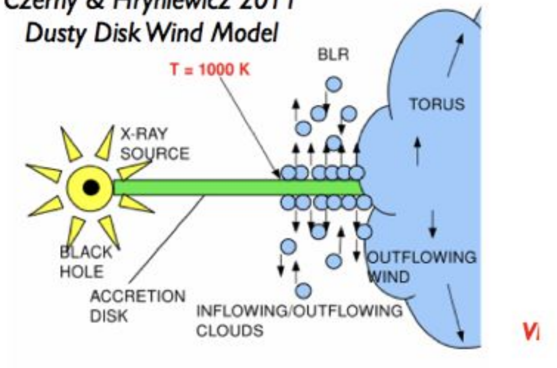

3D model

BH	Disk	BLR	Torus
hrs	days	weeks	months

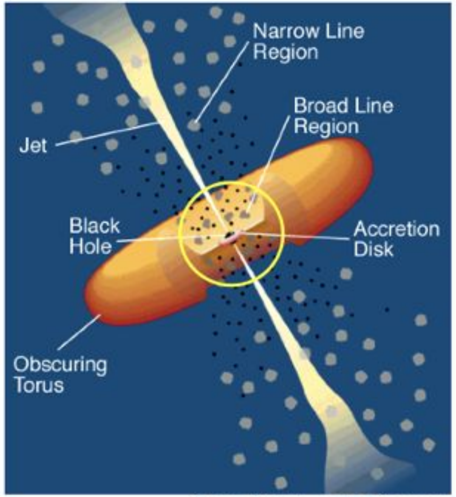

Credit: C.M. Urry and P. Padovani

- **time-delay** between continuum and line flux
- time-delay = size of the broad line region (BLR)

Tornados of whirling space

fast-spinning BH =2 vortices

Vortex 1

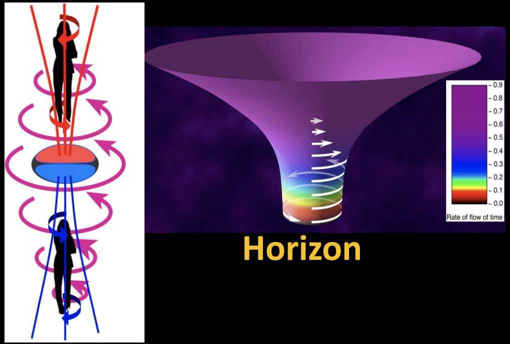

Horizon

Vortex 2

Thorne+20

binary BH = 4 vortices

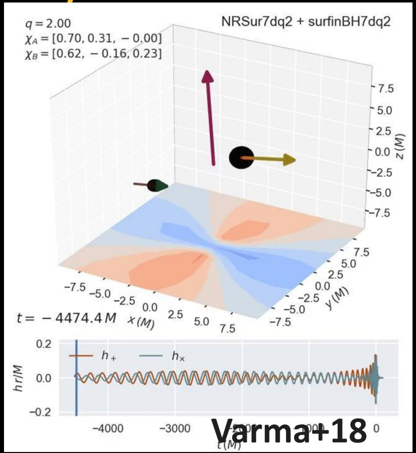

Varma+18

GW from binary SMBH

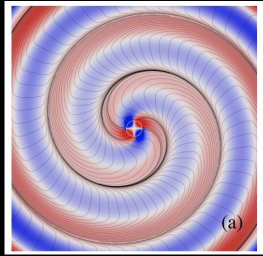

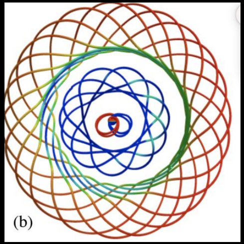

inspiral

head on collison

Perfect storm: Fujiwhara effect

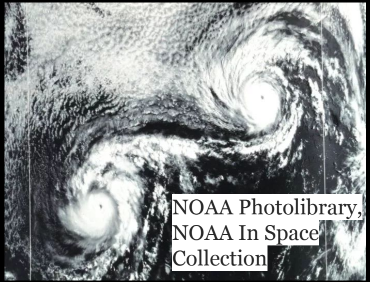

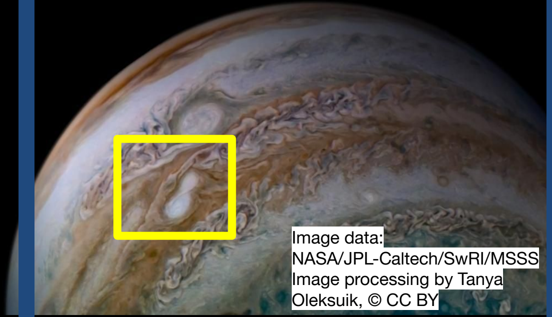

ASTRONOMY MOVIE OF XXI CENTURY: ngEHT mid-2020 production

John Rowe Animation/CSIRO Astronomy and Space Science

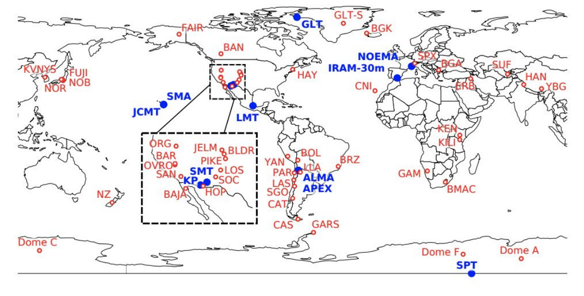

ngEHT potential sites, Raymond+21

"WHERE ARE THEY ?" NAVIGATING PARAMETER HYPERSPACE OF BINARY SMBH

fevol

ftech

f obs

fgeo

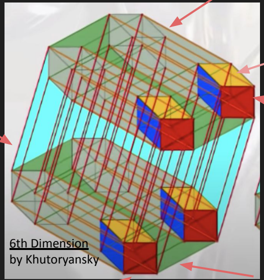

factive

fbin

Pobs=fbin x factive x fgeo x ftech x fevol

Shen&Loeb+10
D'Orazio&Loeb+18

$$P_{\rm obs}(M_{\rm BH}, q, \Delta t, \dot{m}_{\rm Edd}) = \int_{R_{\rm BLR}}^{0.1\,{\rm pc}} P_{\rm obs}(r, M_{\rm BH}, q, \Delta t)\frac{t_{\rm res}(r, M_{\rm BH}, \dot{m}_{\rm Edd})}{r}dr,$$

Jun+13

$$R_{\rm BLR} \approx 2.2\times 10^{-2}\left(\frac{\dot{m}_{\rm Edd}}{0.1}\right)^{1/2}\left(\frac{M_{\rm BH}}{10^8\,M_\odot}\right)^{1/2}\ {\rm pc},$$

$$N_{\rm LISA} = [t_{\rm m}\,/\,t_{\rm Q}]\,f_{\rm Q,b}\mathcal{N}$$

Xin &Haiman +21

$$\mathcal{N} = \int_{m_{\rm min}}^{m_{\rm max}} {\rm d}m \int_{z_{\rm min}}^{z_{\rm max}} {\rm d}z\, f(m,z)\boxed{\phi(M_{1450}(m), z)}\frac{{\rm d}V}{{\rm d}z},$$

QLF Richards+06
Hopkins+07
Shen+20

Ordered Information: Non-Face-on Binaries

Observed Flux ~ Steady mean flux X Doppler boost X Gravitational microlensing X Red noise + Photometric noise

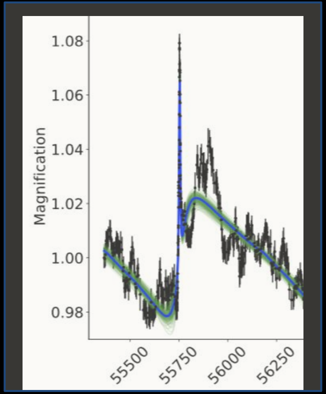

Optical Hu+20

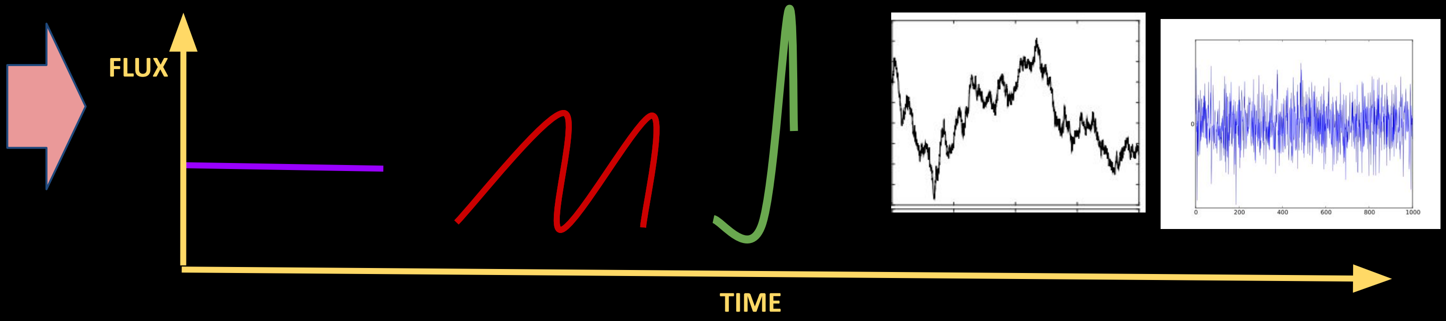

Observed Flux ~ Steady mean flux x (periodic accretion) x Doppler boost x Red noise + Photometric noise

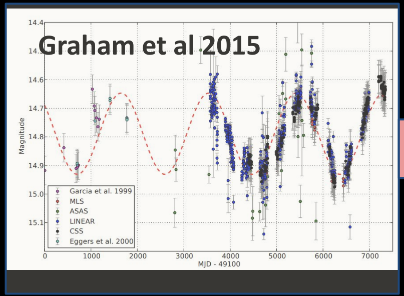

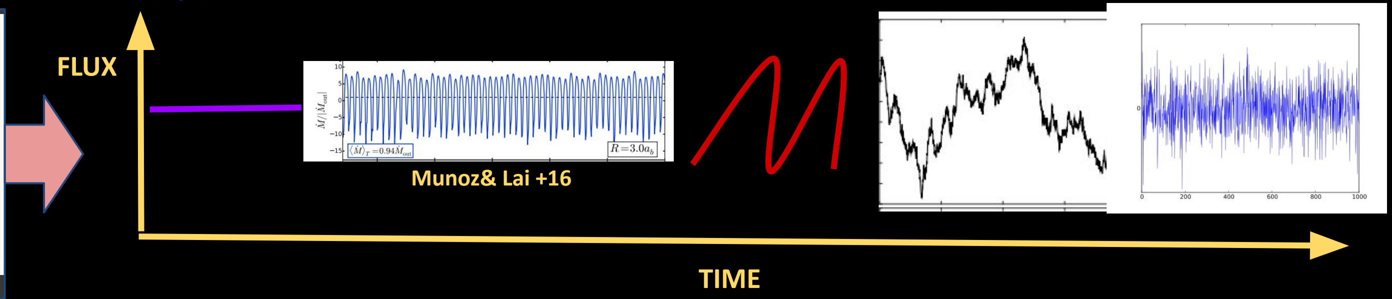

Red Noise: Mimicking ordered information

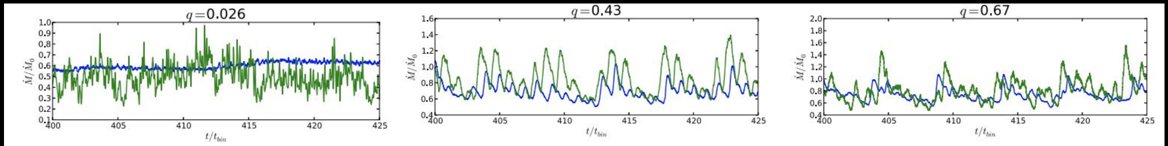

Burst model (Farris+14)

Periodicity signal immersed in red noise

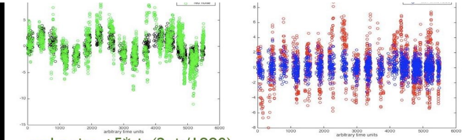

Red Noise mimics periodicity (Vaughan+16)

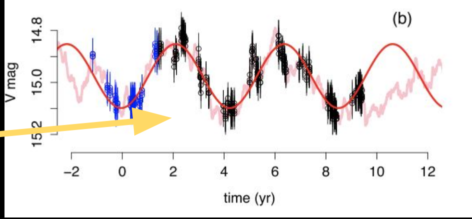

The power spectral density (PSD) for the DRW is (Kelly+09)

$$dX(t) = -\frac{1}{\tau}X(t)dt + \sigma\sqrt{dt}\epsilon(t) + b\,dt, \quad \tau, \sigma, t > 0. \quad (1)$$

$$\mathrm{PSD}(f) = \frac{\tau^2 \mathrm{SF}_\infty^2}{1 + (2\pi f \tau)^2}.$$

$$PSD \propto f^{-2}, for\ f > 1/(2\pi\tau)\ red\,noise$$

$$PSD \propto const(i.e. const \times SF_\infty^2), for\ f < 1/(2\pi\tau)\ white\ noise$$

light crossing time scale

$$t_{\rm lc} = 1.1 \times \left(\frac{M_{\rm BH}}{10^8\,M_\odot}\right)\left(\frac{R}{100R_S}\right) \text{ days},$$

the gas orbital timescale

$$t_{\rm orb} = 104 \times \left(\frac{M_{\rm BH}}{10^8\,M_\odot}\right)\left(\frac{R}{100R_S}\right)^{3/2} \text{ days},$$

accretion disk thermal timescale

$$t_{\rm th} = 4.6 \times \left(\frac{\alpha}{0.01}\right)^{-1}\left(\frac{M_{\rm BH}}{10^8\,M_\odot}\right)\left(\frac{R}{100R_S}\right)^{3/2} \text{ yr},$$

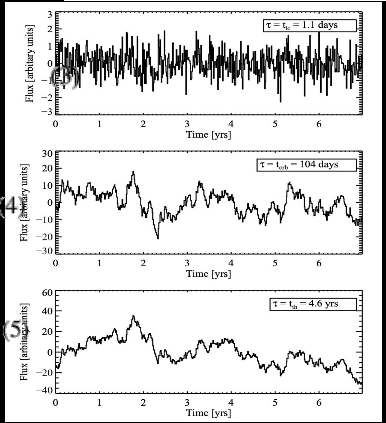

Fourier transform

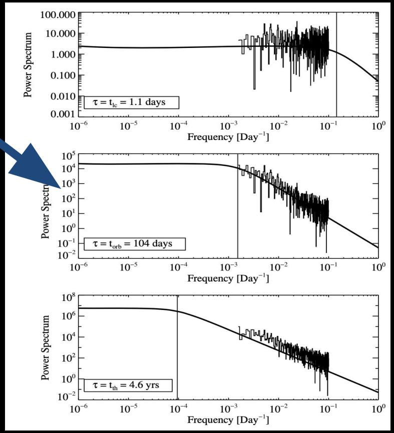

Kelly+09

Under the hood period detection unit: 2D Hybrid method

Under the hood periodicity detection- Sci case (data) supplied by CPG Inkind Team

- preprocessing with DGP, ANN+DGP
- period detection with WWZmatrix coefficients (inhomogenous cadence) + error and significance estimate
- period detection with SUPERLET matrix coefficients (homogenous cadenced LC) + error and significance estimate

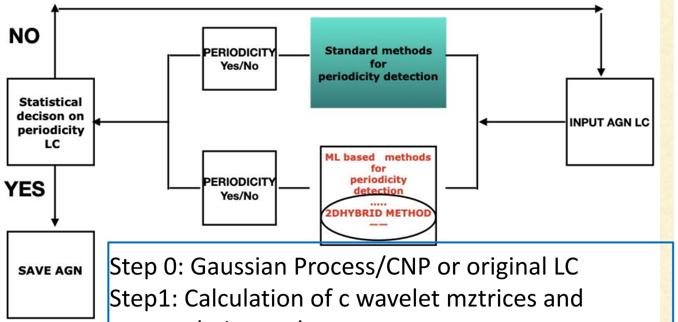

Step 0: Gaussian Process/CNP or original LC
Step1: Calculation of c wavelet mztrices and their envelopes
Step2: Spearman correlation of wavelets envelopes

HYBRID METHOD: 3 STEPS

OUGP=Ornstein–Uhlenbeck Gaussian Process
OUGP(raw LC1)=OUGP1
OUGP(raw LC2)=OUGP2

0 STEP: raw data preprocessing

$$\mathrm{CWT}(a,b) = \frac{1}{\sqrt{2\pi a}} \int_{-\infty}^{+\infty} x(t) \mathrm{e}^{[(t/b)^2/a/2]\beta^2} \mathrm{e}^{\mathrm{i}\omega(t-b)/a} \mathrm{d}t,$$

$$\mathrm{env}(a,b) = \sqrt{\mathrm{Re}\{[\mathrm{CWT}(a,b)]^2\} + \mathrm{Im}\{[\mathrm{CWT}(a,b)]^2\}},$$

I STEP

SpearmanCorrCoeff(env(OUGP1),env(OUGP2)) 2 STEP

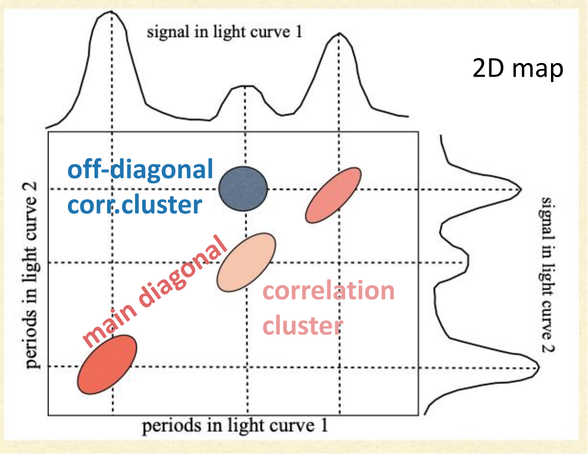

map integration along any period axis

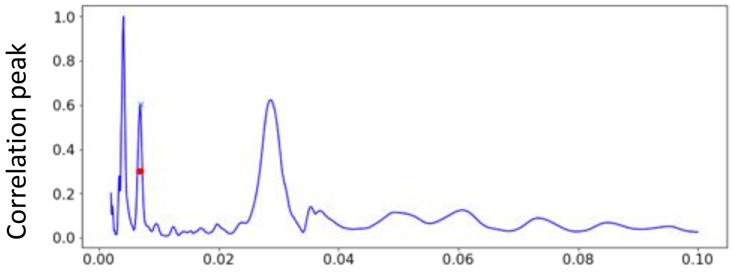

Frequency

Kovačević @ al 2018, 2019, l 2020, 2021

EXAMPLES OF DATA

ARP 102 B

observed:
1987–2010

sampling:

78.1days

77 days

73 days

60 days

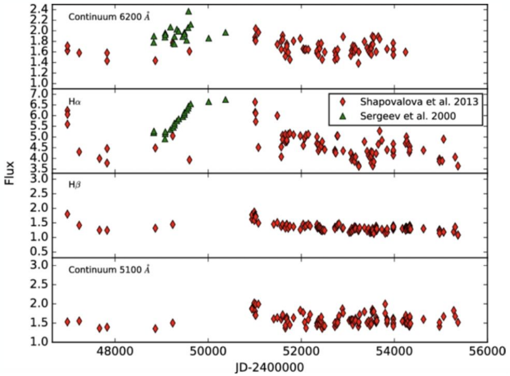

3C 390.3

observed:
1994–2014

sampling:

11.6 days

34.5 days

20.5 days

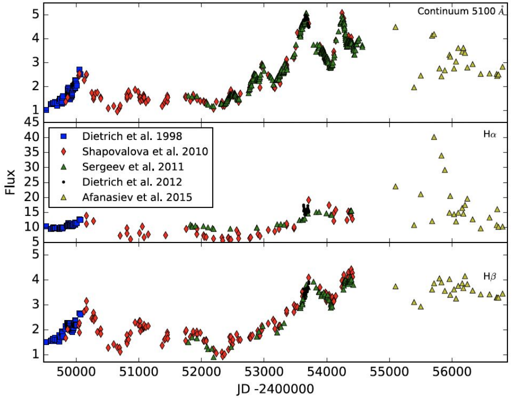

Object name	Type	z	Period	CLC	Sampling (days)	EV	Reference[a]
3C 390.3	BLRG	0.056	1994-2014	Continuum 5100 Å	11.6	0.1623	1, 2, 3, 4, 5
				Hα	34.5	0.1055	
				Hβ	20.5	0.1099	
			1978-1996	Continuum 1370 Å	64.4	0.1737	6, 7
				Lyα	64.4	0.2539	
				CIV	64.4	0.2167	
Arp 102b	LINER	0.024	1987-2010	Continuum 6200 Å	78.1	0.0080	8, 9
				Hα	77.0	0.0245	
				Continuum 5100 Å	73.0	0.0073	8
				Hβ	60.0	0.0090	8
NGC 4151	Seyfert 1	0.003	1993-2006	Continuum 5100 Å	16.1	0.2847	10,11, 12
			1986-2006	Hα	39.6	0.0740	
			1993-2006	Hβ	19.2	0.1367	
NGC 5548	Seyfert 1	0.017	1972-2015	Continuum 5100 Å	6.9	0.0648	13
				Hβ	11.2	0.0917	
E1821+643	Quasar	0.297	1990-2014	Continuum 5100 Å	68.4	0.0357	14
				Hβ	68.4	0.0049	
				Continuum 4200 Å	114.9	0.0359	
				Hγ	114.9	0.0356	

[a] (1) Dietrich et al. (1998), (2) Shapovalova et al. (2010a), (3) Dietrich et al. (2012), (4) Sergeev et al. (2011), (5) Afanasiev et al. (2015), (6) Wamsteker et al. (1997), (7) O' Brien et al. (1998), (8) Shapovalova et al. (2013), (9) Sergeev et al. (2000), (10) Kaspi et al. (1996), (11) Shapovalova et al. (2010b), (12) Bon et al. (2012), (13) Bon et al. (2016), (14) Shapovalova et al. (2016).

NGC 4151

sampling:

16.1 days

39.6 days

19.2 days

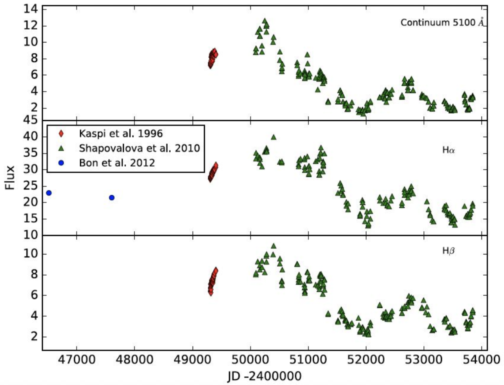

observed:
1993–2006

observed:
1986–2006

observed:
1993–2006

CHECKING RESULTS ON 3 LEVELS

- **1L**>non linear least square fitting of multisinusoidal models to the observed light curves

$$y = \sum_{i=1}^{n} c_i \sin\left(\frac{2\pi t}{p_i} + \phi_i\right) + B.$$

- **2L**>comparison of dynamics of observed light curves and time-series models

MODEL1 (**linearly** coupled oscillators of 2 units)

$$U_a(t) = A(t)\sin(2\pi f_a t + \phi) + cp_{b\to a} \quad (3)$$

$$\times B(t)\sin(2\pi f_b t + 2\pi f_b \tau) + W(t) \quad (4)$$

$$U_b(t) = B(t)\sin(2\pi f_b t) + cp_{a\to b} \quad (5)$$

$$\times A(t)\sin(2\pi f_a t + 2\pi f_a \tau + \phi) + W(t). \quad (6)$$

MODEL 2 (**linearly** coupled oscillators of 3 units)

$$U_a(t) = A(t)\sin(2\pi f_a t + \phi) + cp_{b\to a} \quad (7)$$

$$\times B(t)\sin(2\pi f_b t + 2\pi f_b \tau) + cp_{c\to a} \quad (8)$$

$$\times C(t)\sin(2\pi f_c t + 2\pi f_c \tau_1) + W(t) \quad (9)$$

$$U_c(t) = B(t)\sin(2\pi f_b t) + C(t)\sin(2\pi f_c t) + cp_{a\to b} \quad (10)$$

$$\times A(t)\sin(2\pi f_a t + 2\pi f_a \tau + \phi) + cp_{a\to c} \quad (11)$$

$$\times A(t)\sin(2\pi f_a t + 2\pi f_a \tau_1 + \phi_1) + W(t). \quad (12)$$

- MODEL3 (**nonlinearly** coupled oscillators of 3 units)

$$U_a(t) = A(t)\sin(2\pi f_a t + \phi) + cp_{b\to a} \quad (16)$$

$$\times B(t)\sin(2\pi f_b t + 2\pi f_b \tau) + W(t) \quad (17)$$

$$U_b(t) = B(t)\sin(2\pi f_b t) + cp_{a\to b} \quad (18)$$

$$\times U(t)^2 + W(t) \quad (19)$$

3L of checking: HILBERT TRANSFORM

$$H[x(t)] = \frac{1}{\pi} P \int_{-\infty}^{\infty} \frac{x(\tau)}{t-\tau} d\tau \qquad (3.1)$$

$$z(t) = a(t)e^{j\theta(t)} \qquad (3.3)$$

$$a(t) = \sqrt{x^2(t) + \{H[x(t)]\}^2}, \text{ and } \theta(t) = \arctan\left(\frac{H[x(t)]}{x(t)}\right) \qquad (3.4)$$

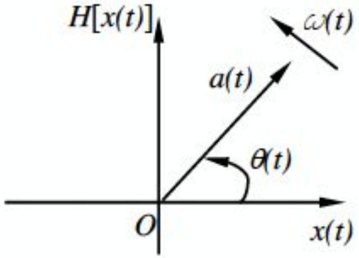

Figure 3.1. Instantaneous Amplitude, Phase Angle and Frequency in Complex Plane

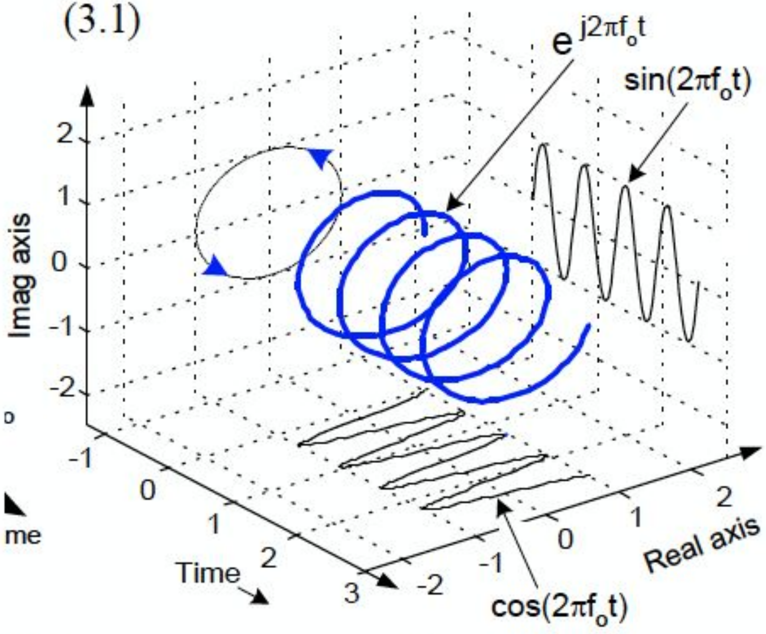

(b)

ARP 102B

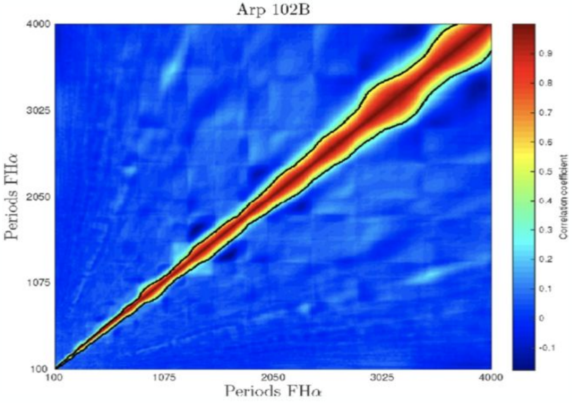

Note the prominent stationarity of the diagonal correlation line and the absence of correlation clusters.

Object name	CLC1	CLC2	$P \pm \Delta P$ (yr)	r	95% CI	p
Arp 102B	Continuum 6200 Å	Hα	–	–	–	
	Continuum 5100 Å	Hβ	–	–	–	

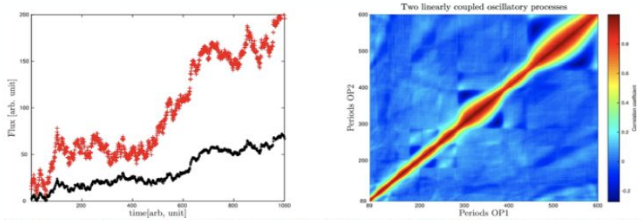

ARP 102B

Simulation of two bidirectional coupled oscillators for the case of Arp 102B. Left: random realization of equation from two time series (black is $U_a = OP1$ and red is $U_b = OP2$) of amplitudes $A = 5.29$, $B = 1.99$, phase $\phi = 0.4174$ rad, coupling strengths $cp_{a\to b} = 0.4$, $cp_{b\to a} = 0.2$, time delay is 100 and periods are 500 and 300 arbitrarily chosen time units. Right: corresponding 2D correlation map.

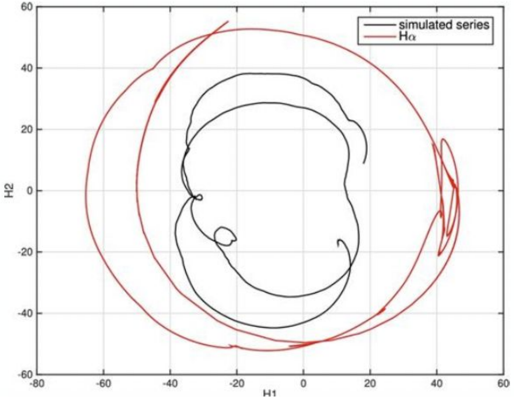

Both curves are similar and non-closed, indicating either weak coupling or the absence of periodicity. They appear to intersect themselves due to projection on to 2D phase space.

$$U_a(t) = A(t) \cdot \sin(2\pi f_a t + \phi) + cp_{b\to a} \cdot B(t) \cdot \sin(2\pi f_b t + 2\pi f_b \tau) + W(t)$$

$$U_b(t) = B(t) \cdot \sin(2\pi f_b t) + cp_{a\to b} \cdot A(t) \cdot \sin(2\pi f_a t + 2\pi f_a \tau + \phi) + W(t)$$

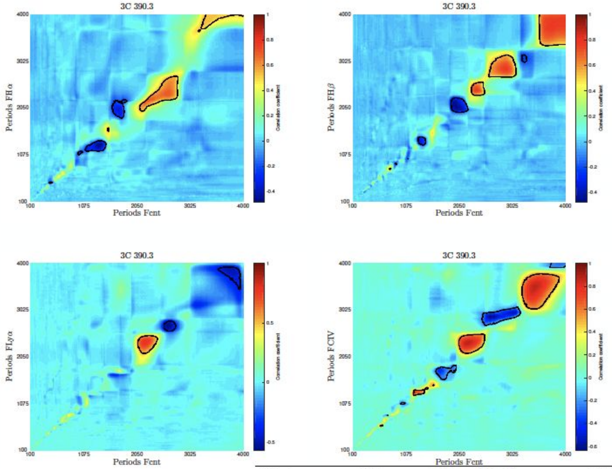

Object name	CLC1	CLC2	$P \pm \Delta P$ [yr]	r	95%CI	p
3C 390.3	Continuum 5100 Å	Hα	9.5 ± 0.3	0.5	(0.49,0.51)	< 0.00001
			7.2 ± 1.2	0.69	(0.68,0.7)	< 0.00001
			6.3 ± 0.9	0.68	(0.67,0.69)	< 0.00001
			4.0 ± 0.04	-0.47	(-0.48,-0.45)	< 0.00001
			5.44 ± 0.1	-0.35	(-0.37,-0.33)	< 0.00001
		Hβ	10.11 ± 0.1	0.77	(0.76,0.78)	< 0.00001
			7.67 ± 0.02	0.71	(0.7,0.72)	< 0.00001
			6.42 ± 1.6	0.75	(0.74,0.76)	< 0.00001
			5.43 ± 0.8	-0.47	(-0.48,-0.45)	< 0.00001
			3.6 ± 0.4	-0.33	(-0.35,-0.31)	< 0.00001
	Continuum 1370 Å	Lyα	10.34 ± 0.1	-0.47	(-0.49,-0.45)	< 0.00001
			7.1 ± 0.02	-0.53	(-0.54,-0.51)	< 0.00001
			6.25 ± 1.42	0.77	(0.76,0.78)	< 0.00001
		CIV	9.42 ± 0.02	0.85	(0.84,0.86)	< 0.00001
			7.84 ± 0.02	-0.6	(-0.61,-0.59)	< 0.00001
			6.4 ± 1.22	0.85	(0.84,0.86)	< 0.00001
			4.68 ± 0.7	-0.42	(-0.44,-0.40)	< 0.00001
			3.4 ± 0.4	0.75	(0.74,0.76)	< 0.00001

3C 390.3

2L of CHECKING: simulations of coupled oscillators

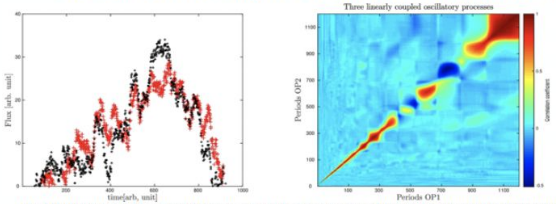

Figure 12. Simulation of bidirectional coupled three oscillators network for the case of 3C 390.3. Left: Random realization of Eq. (4) form two time series (black is $U_a = OP1$, and red is $U_c = OP2$) of amplitudes $A = 1.954, B = 1.729, C = 2.357$, phase $\phi = \phi_1 = 2.359$ rad coupling strengths $cp_{a\to b} = 0.7, cp_{a\to c} = 0.5, cp_{b\to a} = 0.2, cp_{c\to a} = 0.3$, frequencies $f_a = \frac{1}{1000}, f_b = \frac{1}{300}, f_c = \frac{1}{100}$, and time delay of 100 arbitrary chosen time unites. Right: corresponding 2D correlation map, which clearly shows three clusters related to fundamental periods as well as clusters of negative correlation.

Simulation of bidirectional coupled three-oscillator network for the case of 3C 390.3.

$$
\begin{aligned}
U_a(t) = {} & A(t)\cdot\sin(2\pi f_a t + \phi) + cp_{b\to a}\cdot \\
& B(t)\cdot\sin(2\pi f_b t + 2\pi f_b \tau) + cp_{c\to a}\cdot \\
& C(t)\cdot\sin(2\pi f_c t + 2\pi f_c \tau_1) + W(t) \\
U_c(t) = {} & B(t)\cdot\sin(2\pi f_b t) + C(t)\cdot\sin(2\pi f_c t) + cp_{a\to b}\cdot \\
& A(t)\cdot\sin(2\pi f_a t + 2\pi f_a \tau + \phi) + cp_{a\to c}\cdot \\
& A(t)\cdot\sin(2\pi f_a t + 2\pi f_a \tau_1 + \phi_1) + W(t)
\end{aligned}
$$

3L of checking: Hilbert transform

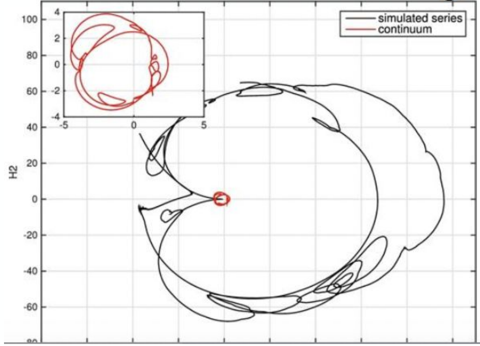

Comparison of the phase trajectories between the continuum of 3C 390.3 and simulated curve OP1 from the oscillatory network model

$$y^{\mathrm{H}}(t) = \frac{1}{\pi} PV \int_{-\infty}^{\infty} \frac{y(t)}{t-\tau} \mathrm{d}\tau$$

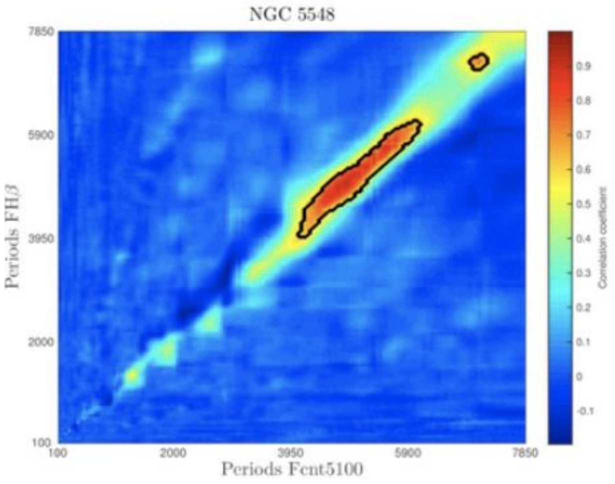

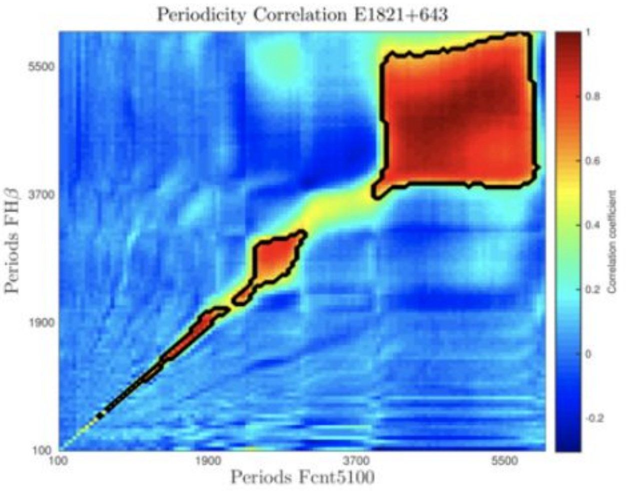

BINARY SMBH CANDIDATES

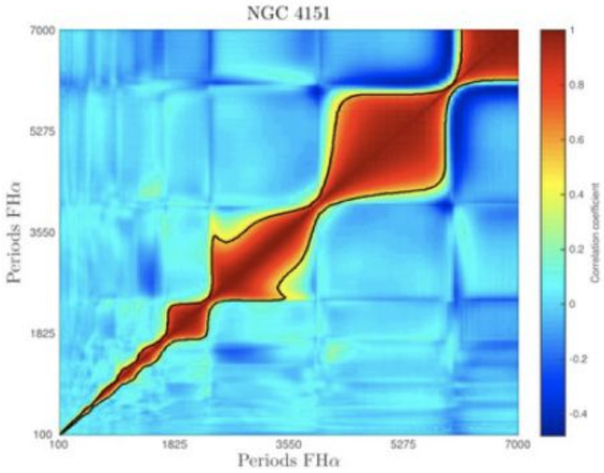

NGC 4151	Continuum 5100 Å	Hα	13.76 ± 3.73	0.96	(0.956,0.962)	< 0.00001
			8.33 ± 2.33	0.97	(0.968,0.972)	< 0.00001
			5.44 ± 1.29	0.98	(0.978,0.981)	< 0.00001
NGC 5548	Continuum 5100 Å	Hβ	13.3 ± 2.26	0.87	(0.867,0.873)	< 0.00001
E1821+643	Continuum 5100 Å	Hβ	12.76 ± 5.6	0.98	(0.979,0.981)	< 0.00001
			6.93 ± 1.99	0.80	(0.792,0.808)	< 0.00001
			4.75 ± 0.79	0.80	(0.792,0.808)	< 0.00001
	Continuum 4200 Å	Hγ	12.36 ± 6.1	0.99	(0.989,0.991)	< 0.00001
			6.52 ± 3.26	0.91	(0.906,0.914)	< 0.00001
			4.34 ± 0.74	0.94	(0.937,0.943)	< 0.00001

NGC 4151

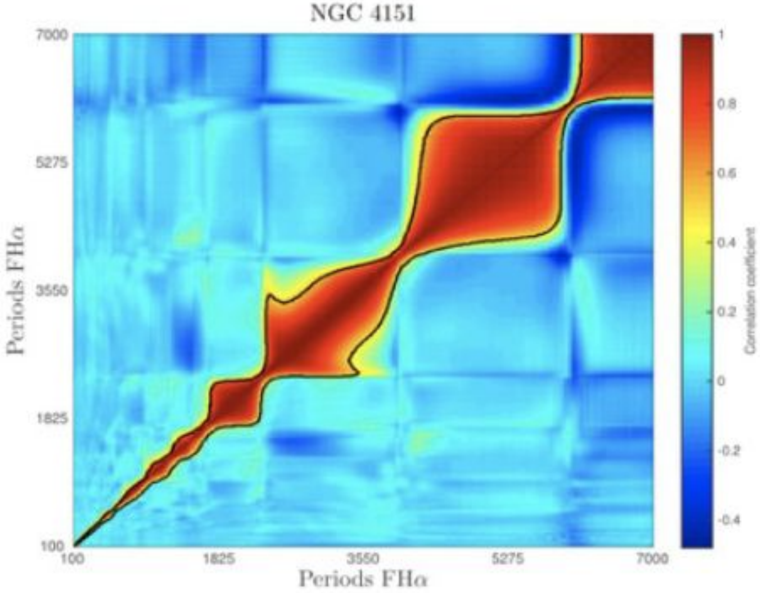

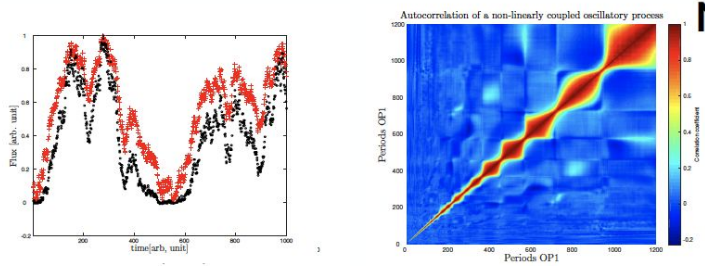

Figure 16. Simulation of two bidirectional coupled oscillators for the case of NGC 4151. Left: Random realization of Eq. (8) form two time series (black is $U_a = OP1$, and red is $U_b = OP2$) of amplitudes $A = 6.09, B = 1.04$, phase $\phi = 2.2\ rad$, coupling strengths $cp_{a\to b} = 0.7, cp_{b\to a} = 0.6$, periods are 500, 300 and time delay is 100 arbitrarily chosen time units. Note the similarity of sharpness of this signal 'bursts' with features in the observed light curves. Right: corresponding 2D correlation map .

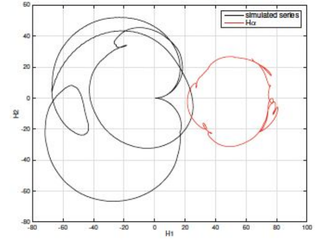

Figure 17. As in Fig. 13 but for the Hα line of NGC 4151 and simulated OP1 curve described by Eq. (8) with parameter values as in (see Fig. 16). Note that phase curve of Hα line is shifted by + 50 units on x axis for a better view.

$$
\begin{aligned}
U_a(t) &= A(t)\cdot\sin(2\pi f_a t + \phi) + cp_{b\to a}\cdot \\
&\quad B(t)\cdot\sin(2\pi f_b t + 2\pi f_b \tau) + W(t) \\
U_b(t) &= B(t)\cdot\sin(2\pi f_b t) + cp_{a\to b}\cdot \\
&\quad U_a(t)^2 + W(t)
\end{aligned} \tag{8}
$$

where the non-linear coupling is introduced by squared term $U_a(t)^2$. Simulated curves consists of sum and multiple of base sinus signals of periods of 500 and 300 arbitrary chosen time units. As a consequence, periods of $2*500, 2*300, 500, 300$ are accompanied with an interference patterns $500+300, 500-300$ (right plot in Fig. 16). Comparing this scenario with autocorrelation of periods in Hα (see Fig. 7), the largest period of 13.76 yr can be interpreted as interference pattern (i.e. sum) of two smaller periods of 5.44 and 8.33 yr.

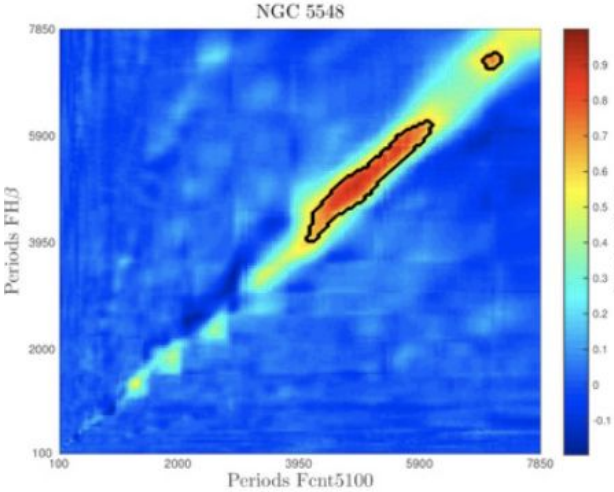

NGC 5548

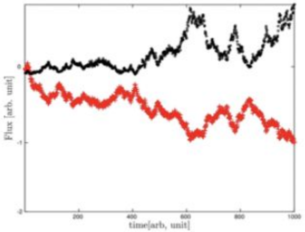

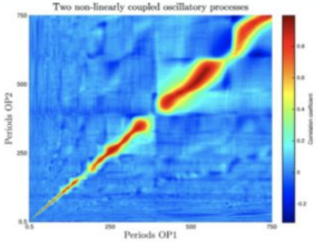

Simulation of two bidirectional coupled oscillators for the case of NGC 5548. Left: random realization of equation (19) from two time series (black is $U_a = OP1$ and red is $U_b = OP2$) of amplitudes $A = 5.92$, $B = 1.27$, phases $\phi = 2.65$ rad, coupling strengths $cp_{a\to b} = 0.7$, $cp_{b\to a} = 0.2$, periods 500 and 300 and time delay is 100 arbitrarily chosen time units

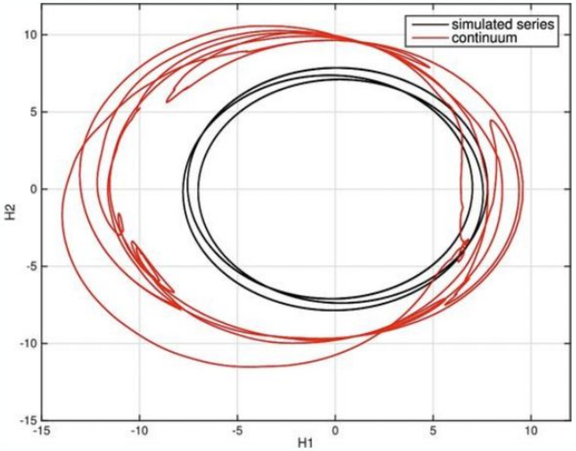

Note the chaotic-like appearance of both curves.

$$U_a(t) = A(t)\sin(2\pi f_a t + \phi) + cp_{b\to a} \tag{16}$$

$$\times B(t)\sin(2\pi f_b t + 2\pi f_b \tau) + W(t) \tag{17}$$

$$U_b(t) = B(t)\sin(2\pi f_b t) + cp_{a\to b} \tag{18}$$

$$\times U_a(t)^2 + W(t). \tag{19}$$

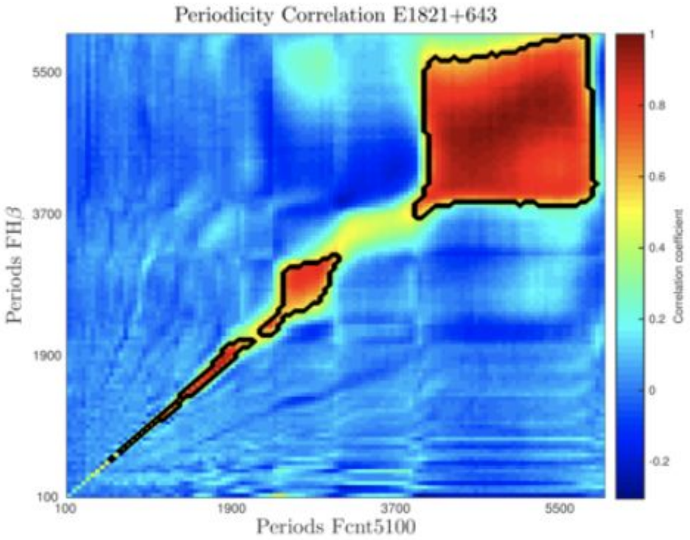

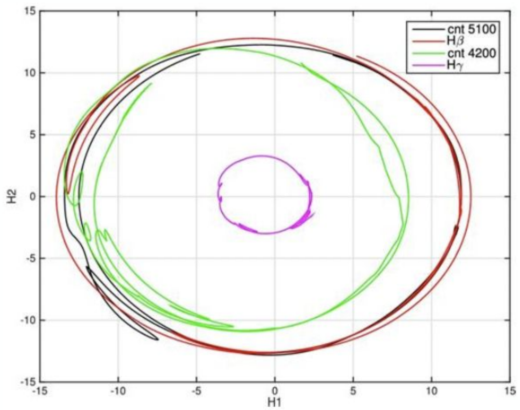

NGC E1821+643

Its 2D correlation maps are similar to the case of NGC 4151. Particularly, if we look at phase portraits of the light curves normal limit cycles are observed in the dynamics of E1821 + 643. They are similar to the phase portrait of regular sinusoids. We note the presence of two smaller elongated loops in all phase curves reflecting two smaller periods.

Lyapunov Exponents & Recurrence Analysis: Quasar vs. Sinusoidal Signal

Fatovic et al +23

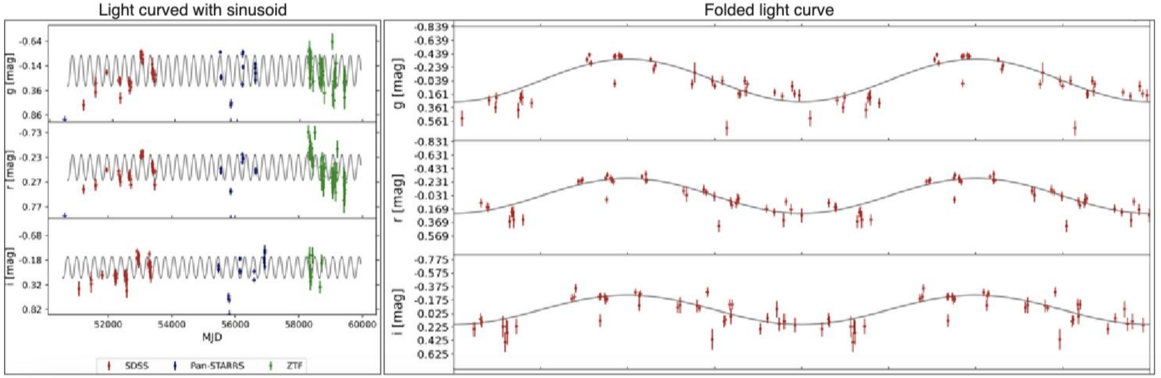

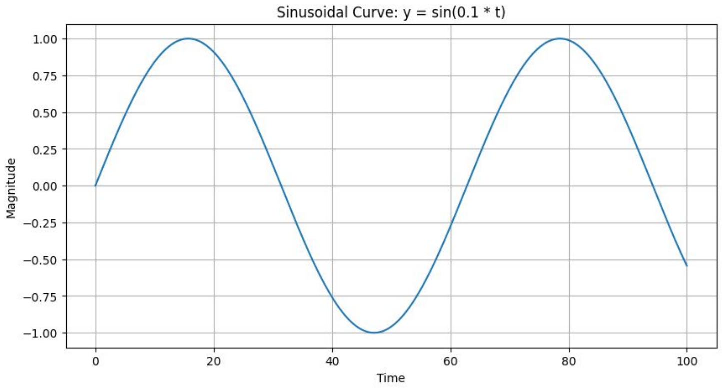

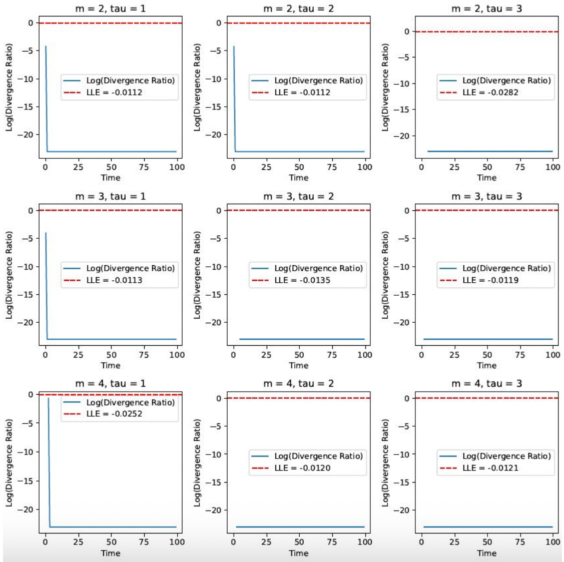

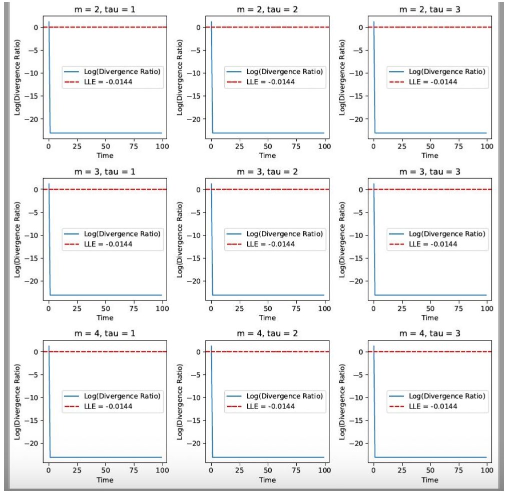

Complex Dynamics in Quasar Light Curves: A Recurrence Analysis Perspective

Pure Sinusoid

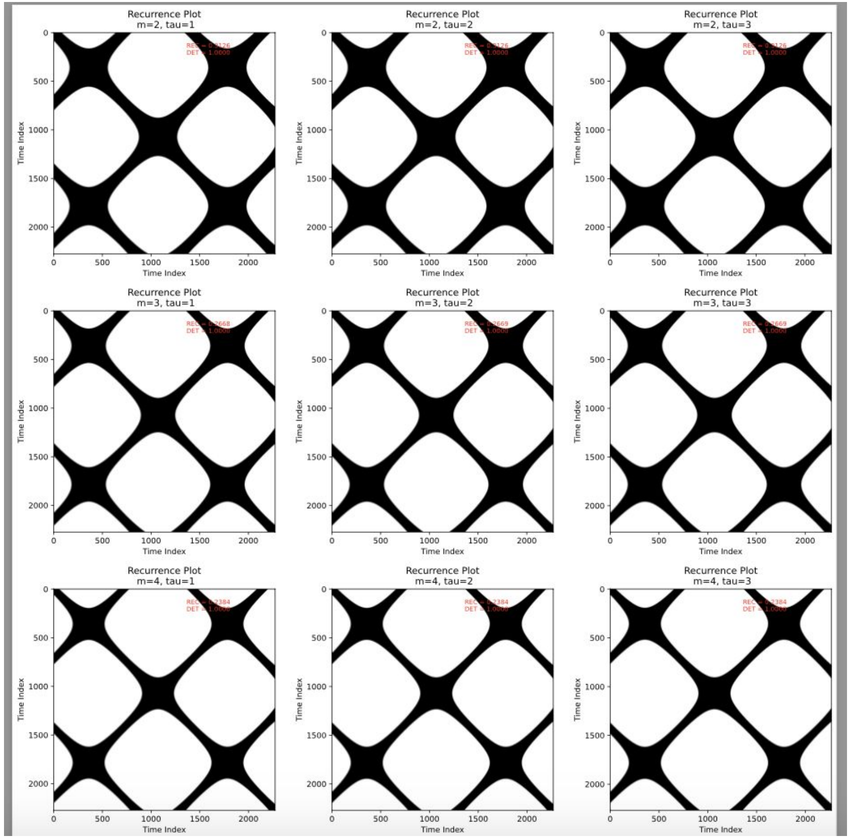

Quasar light curve

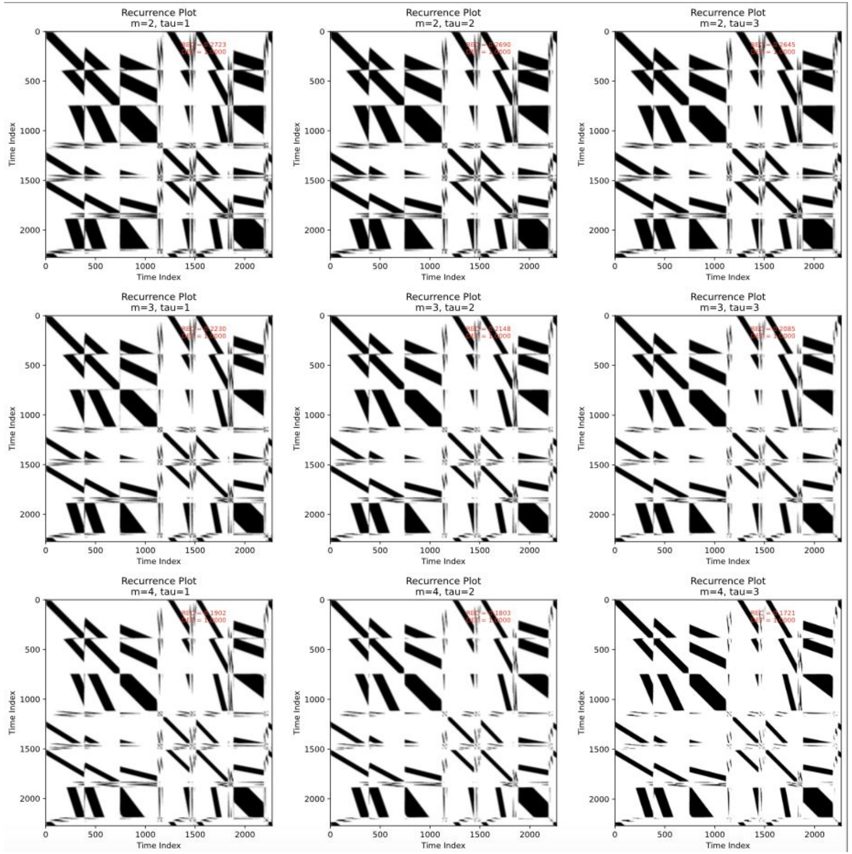

SUMMARY

- The integration of astronomical big data surveys with upcoming nHz GW observations is essential for revealing binary SMBH.
- The application of advanced methods on new astronomical big data can facilitate the detection of binary SMBH systems
- Given the intricacy of both binary and single AGN light curves, there's an emerging need for innovative observables (NOb).
- Novel methods, such as our 2D Hybrid approach, can detect periodicity of binary SMBH within a 2D correlation signal space, representing a potential NOb.
- Our recent pilot experiments using recurrence analysis of newly detected binary SMBH have indicated the stability and periodic signal characteristics of the observed object.